Mace et al., SUPPLEMENTARY FIGURES AND REFERENCES

SUPPLEMENTARY FIGURES 1–9

SUPPLEMENTARY REFERENCE

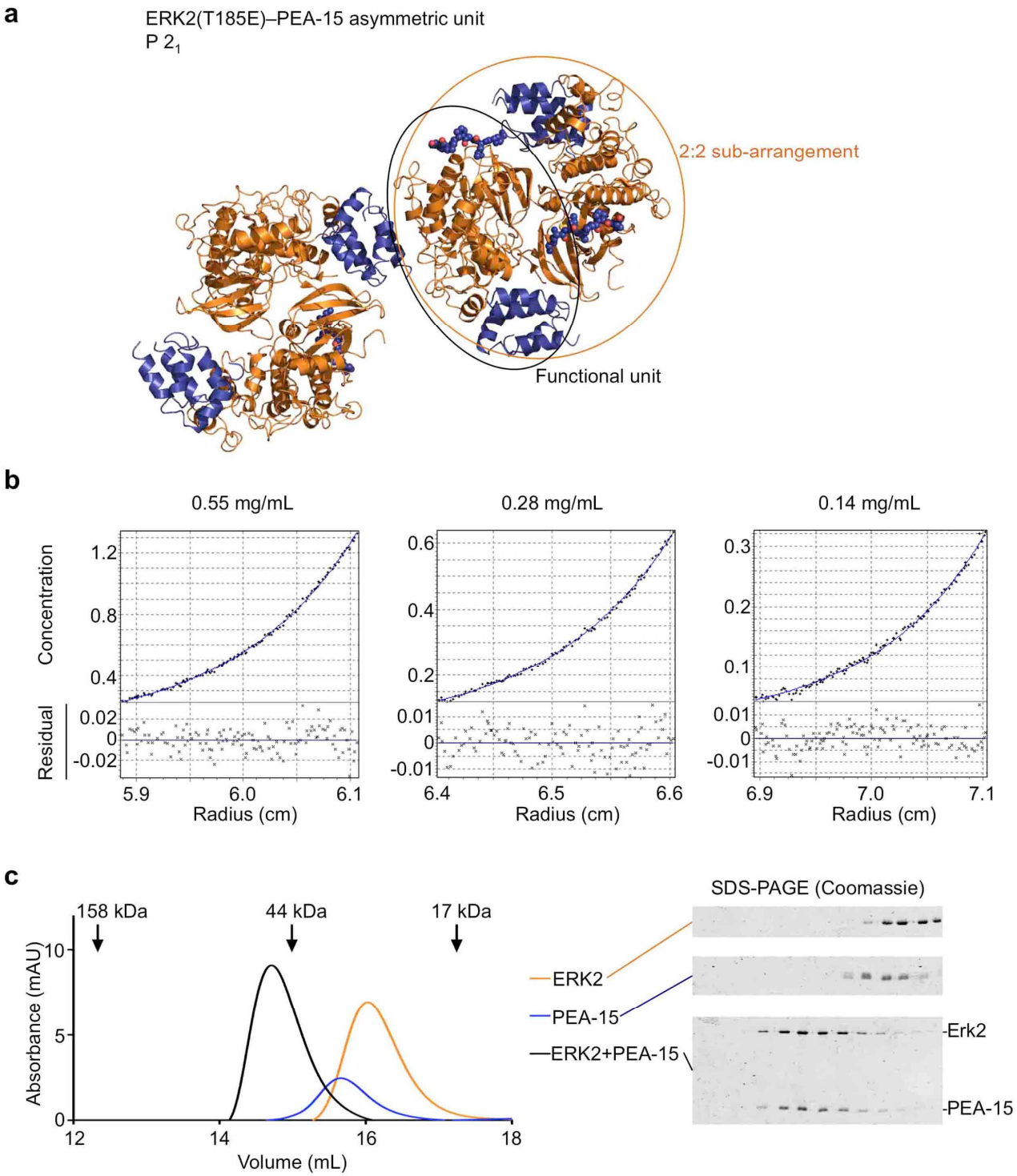

Supplementary Figure S1. Asymmetric unit and 1:1 ERK2(T185E)–PEA-15 complex in solution. (a) Crystallographic asymmetric unit observed in the structure of ERK2(T185E) (orange) bound to full-length PEA-15 (blue; death effector domain in ribbon and C-terminal segment in spheres respectively). Indicated are the 2:2 sub-arrangements (orange circle) and the single 1:1 complex arrangement (black circle) depicted in **Fig. 1a**. Of note, connectivity between the DED and the C-terminal segment cannot be unambiguously established since the PEA-15 linker regions are not defined. (**b**) Sedimentation equilibrium analytical ultracentrifugation of full-length PEA-15 with ERK2(T185E). The complex exhibits a molecular weight of 53.4 kDa, virtually identical to the expected molecular weight for a 1:1 complex of 56.5 kDa. (**c**) Size-exclusion chromatography. Left: Size-exclusion chromatography of ERK2, PEA-15 and the complex (orange, blue and black respectively). The apparent molecular weight of 55.3 kDa obtained from size-exclusion chromatography is also in accordance with a 1:1 arrangement. Right: SDS-PAGE of peak fractions from size-exclusion chromatography experiments stained with Coomassie blue.

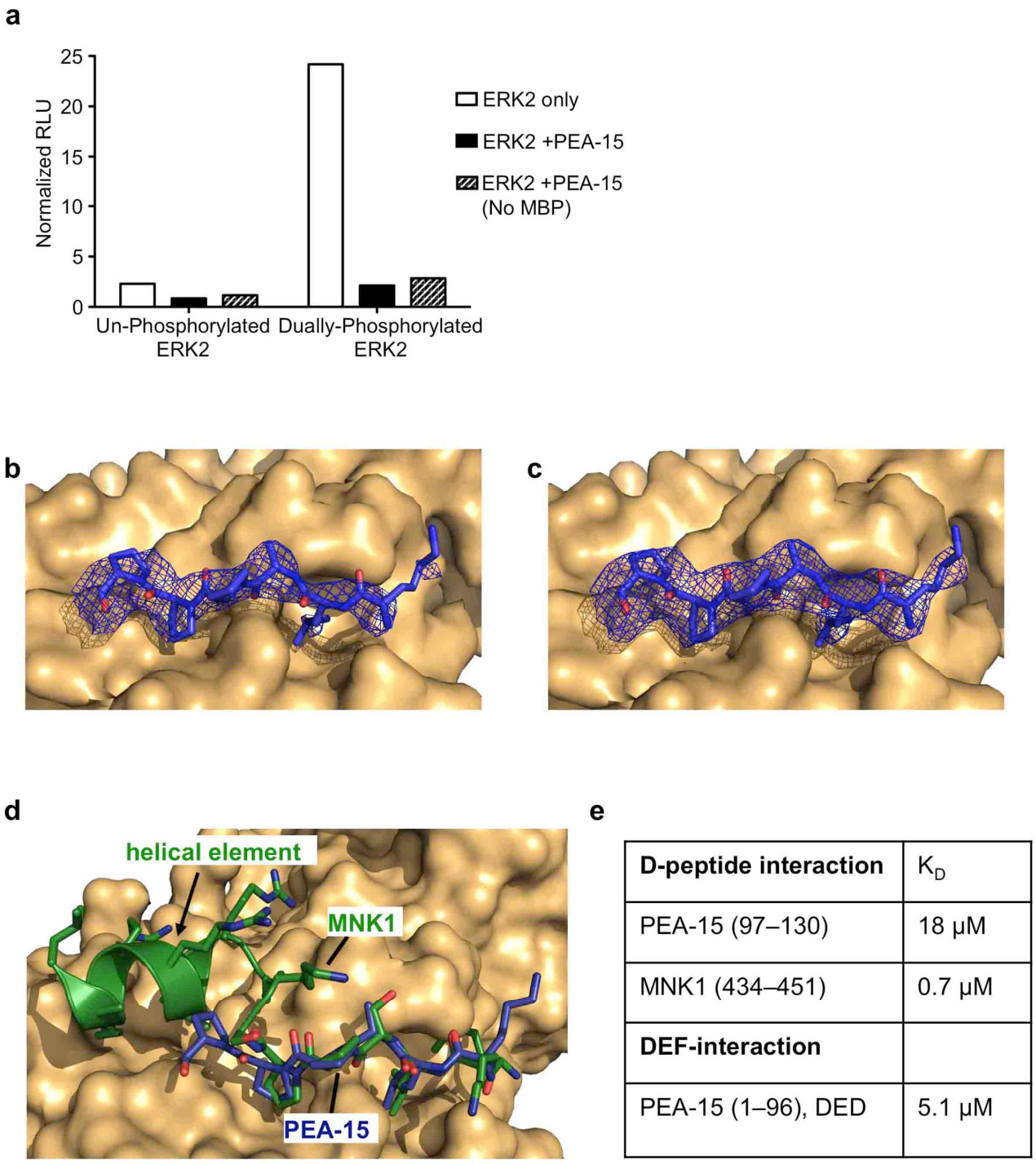

D-peptide interaction	K_D
PEA-15 (97–130)	18 μM
MNK1 (434–451)	0.7 μM
DEF-interaction	
PEA-15 (1–96), DED	5.1 μM

Supplementary Figure S2. Bipartite binding of PEA-15 to ERK2: Inhibition, D-peptide binding and relative contributions of PEA-15 interaction motifs. (a) Inhibition of ERK2 catalytic activity determined by measuring phosphorylation of the general substrate myelin basic protein (MBP). Shown is quantification of the luminescence from an ADP-glo kinase activity assay with unphosphorylated and dually phosphorylated ERK2 in the presence and absence of PEA-15. **(b-d)** D-peptide interaction. The ERK2 D-peptide binding region is shown in surface representation with bound PEA-15 C-terminal segment (residues 122-127; blue; stick representation). Additionally shown in (**b**) is a 2Fo-Fc omit electron density map (contoured at 1σ) for the C-terminal segment (i.e. the map was calculated without phasing contribution from the model comprising the C-terminal segment). In (**c**) the final 2Fo-Fc electron density map (contoured at 1σ) is shown for the C-terminal segment. Panel (**d**) shows an overlay of the PEA-15 C-terminal segment with the MNK1 D-peptide (residues 435-450) from the recent MNK1 peptide-ERK2 structure (PDB entry 2Y9Q). (**e**) Relative binding contributions of the two PEA-15 interaction motifs in the bi-partite interaction of ERK2. Shown are dissociation constants from ITC measurements for the D-peptide- vs. DEF-site interaction of PEA15 with non-phosphorylated ERK2. The K_D for the MNK1 D-peptide interaction with ERKs as reported by Garai *et al.*[25] is also included for comparison.

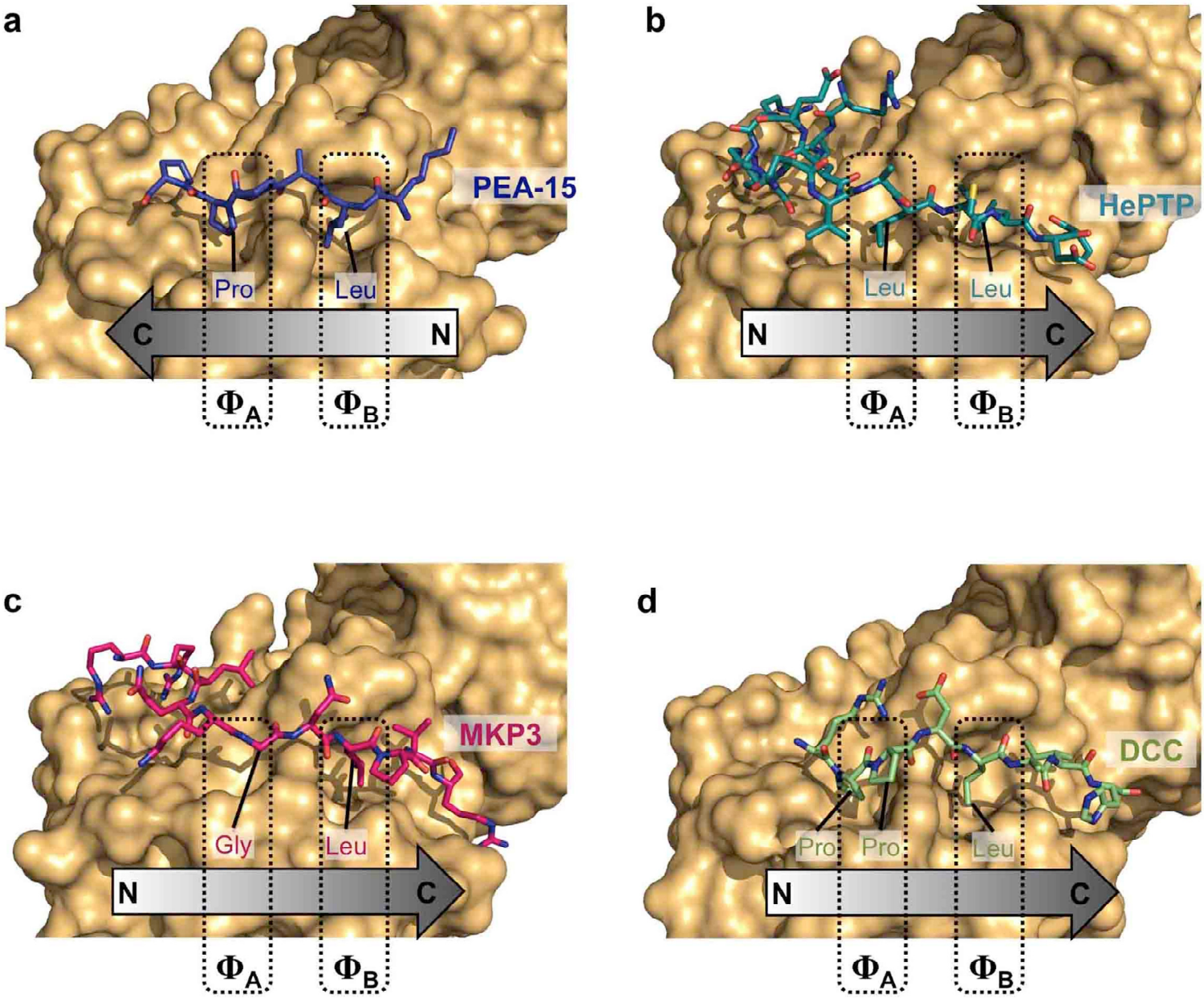

Supplementary Figure S3. Comparison of the binding mode observed for the PEA-15 C-terminal segment with available ERK2–D-peptide complexes. (a) Binding mode of the C-terminal segment of PEA-15 in complex with ERK2 (directionality indicated). (**b–d**) Equivalent views of peptides from hematopoietic protein tyrosine phosphatase (HePTP[23]), MAP kinase phosphatase 3 (MPK3[24]) and the Netrin-receptor 'deleted in colorectal cancer' (DCC[22]) in complex with ERK2 (cyan, magenta and green respectively, PDB accession numbers: 2gph, 2fys, 3o71). Residues occupying the Φ_A and Φ_B pockets are indicated.

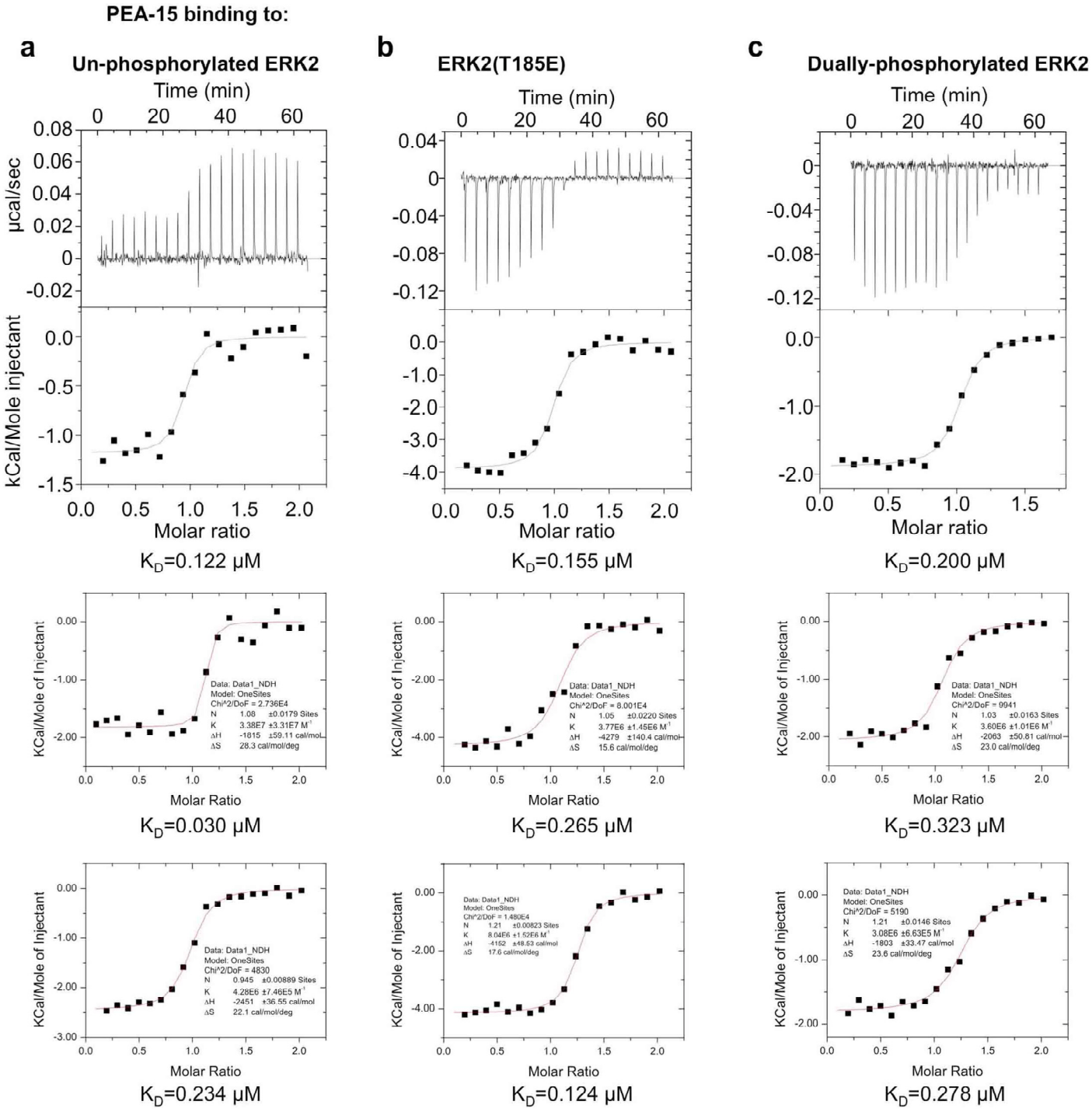

d

ERK2 variant	Average K_D	Standard error of the mean (3 experiments)
Un-phosphorylated	0.129 µM	0.059 µM
T185E	0.155 µM	0.043 µM
Dually-phosphorylated	0.270 µM	0.033 µM

Supplementary Figure S4. Isothermal titration calorimetry of PEA-15 binding to different activation states of ERK2. ITC titrations (in triplicate) are shown for the binding of full-length PEA-15 to (**a**) unphosphorylated ERK2, (**b**) ERK2(T185E) (threonine phosphomimetic ERK2), and (**c**) dually phosphorylated ERK2. (**d**) Average K_D-values and standard errors of the mean derived from panels a-c are shown for the different complexes. PEA-15 shows a binding affinity suggestive of a regulatory interaction.

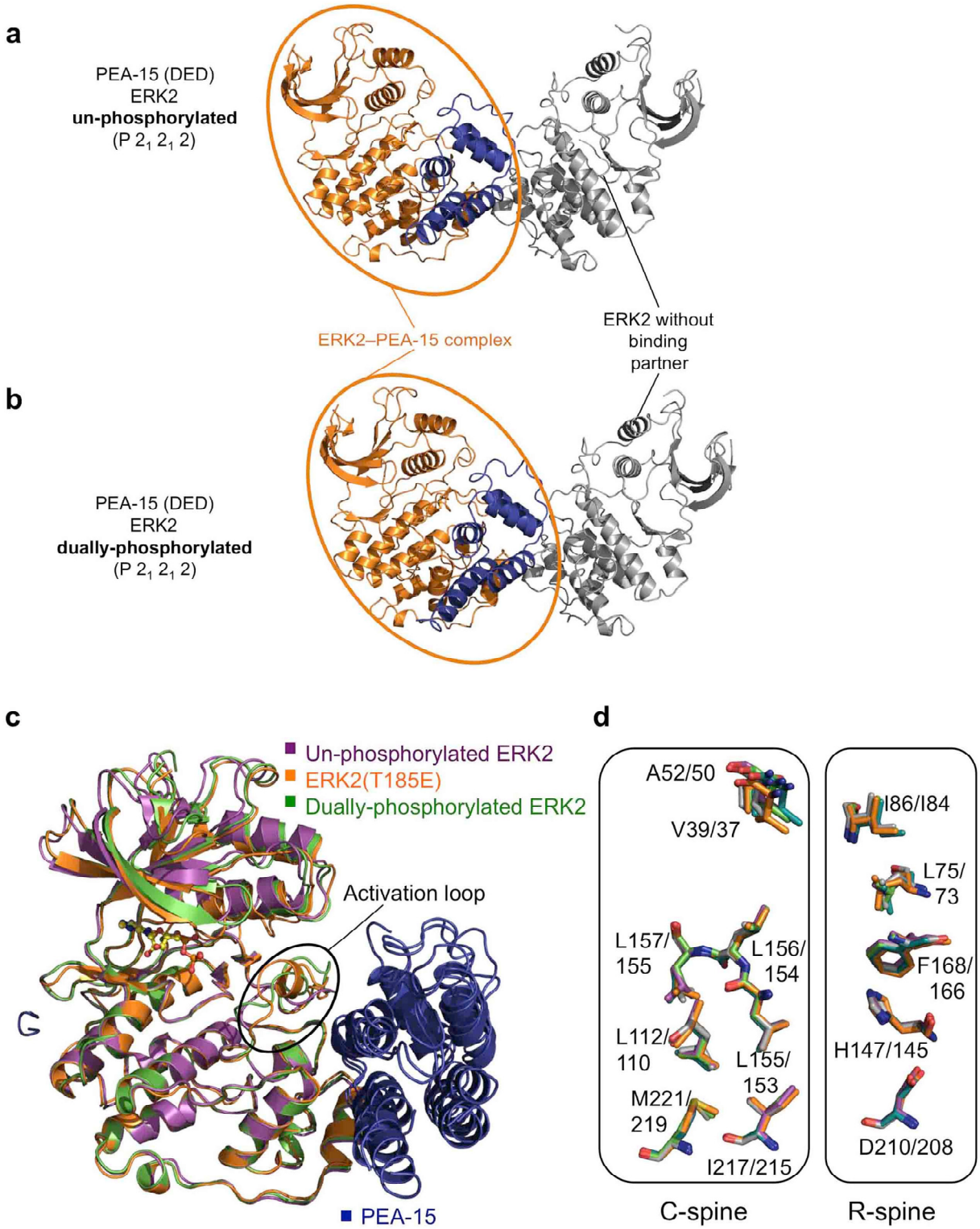

Supplementary Figure S5. Structures of unphosphorylated and dually phosphoryalted ERK2–PEA-15 DED complexes. Crystallographic asymmetric units are shown for the structures of the PEA-15 death effector domain in complex with (**a**) un-phosphorylated ERK2 and (**b**) dually phosporylated ERK2. The crystal packing (space group P21212) of both structures results in each asymmetric unit containing one ERK2-PEA-15 complex (orange circle) and one ERK2 molecule lacking a binding partner (grey). (**c**) Overlay of the three complex structures. The PEA-15 death effector domain (blue) binds in identical modes to the DEF docking-region of unphosphorylated ERK2 (magenta), ERK2(T185E) (orange) and dually phosphorylated ERK2 (green). (**d**) residues constituting the catatlytic and regulatory spines defined based on Kornev *et. al.* [52] are displayed in stick representation for the overlaid complexes (as in c) and additionally for unbound un-phosphorylated and dually phosphorylated ERK2 (grey, PDB: 1ERK and teal, PDB: 2ERK, respectively). The overlay shows that these residues are nearly identical in the five different ERK2 structures (residue numbers are displayed for human/rat ERK2).

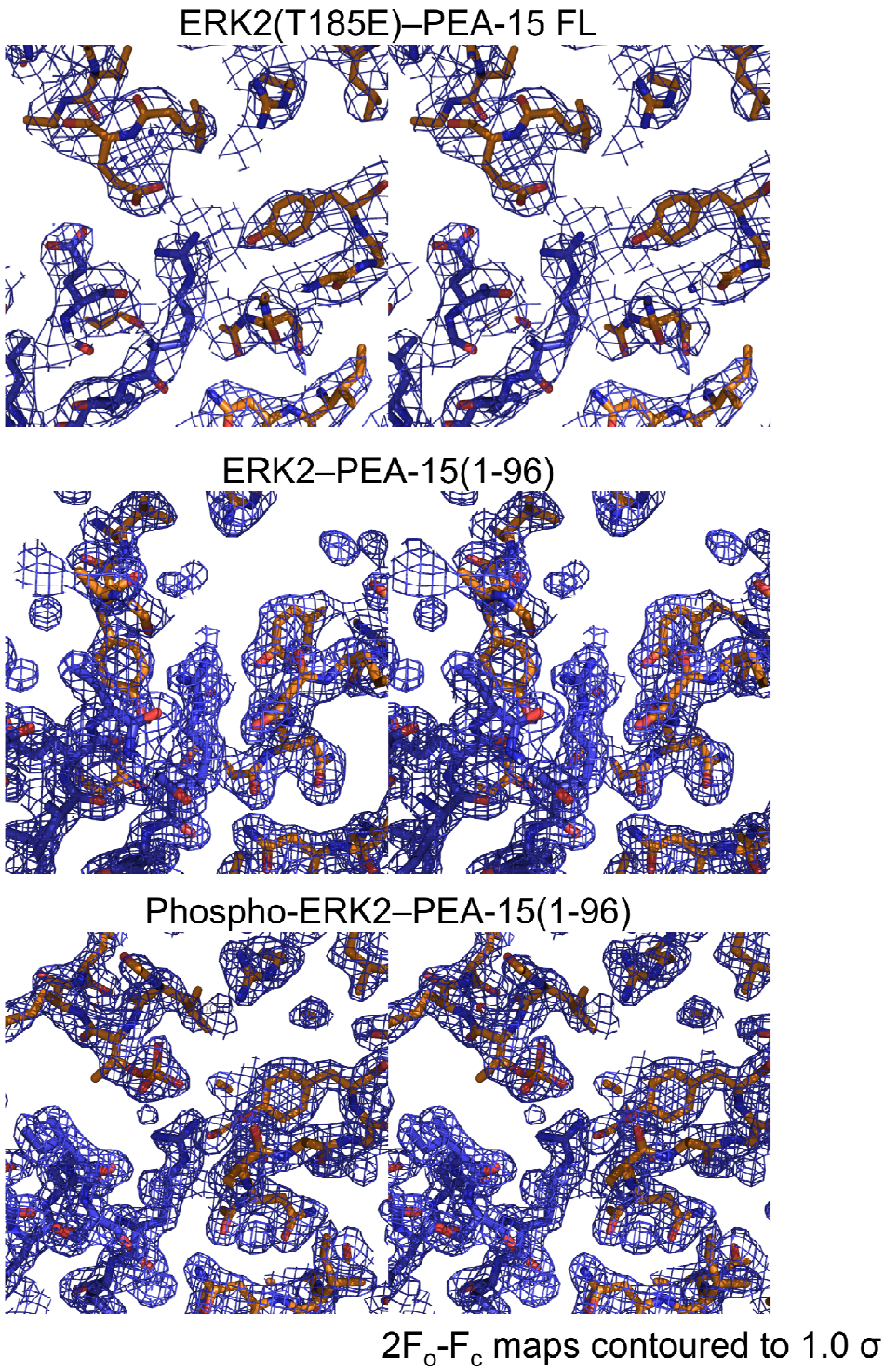

Supplementary Figure S6. Stereo view of representative electron density maps of the three PEA-15–ERK2 complex structures. Sections of each structure, centered on the crucial binding residue Arg71 of PEA-15, are shown as sticks with PEA-15 residues colored blue and ERK2 residues colored orange. $2F_o–F_c$ maps for each region are shown contoured to 1.0 σ.

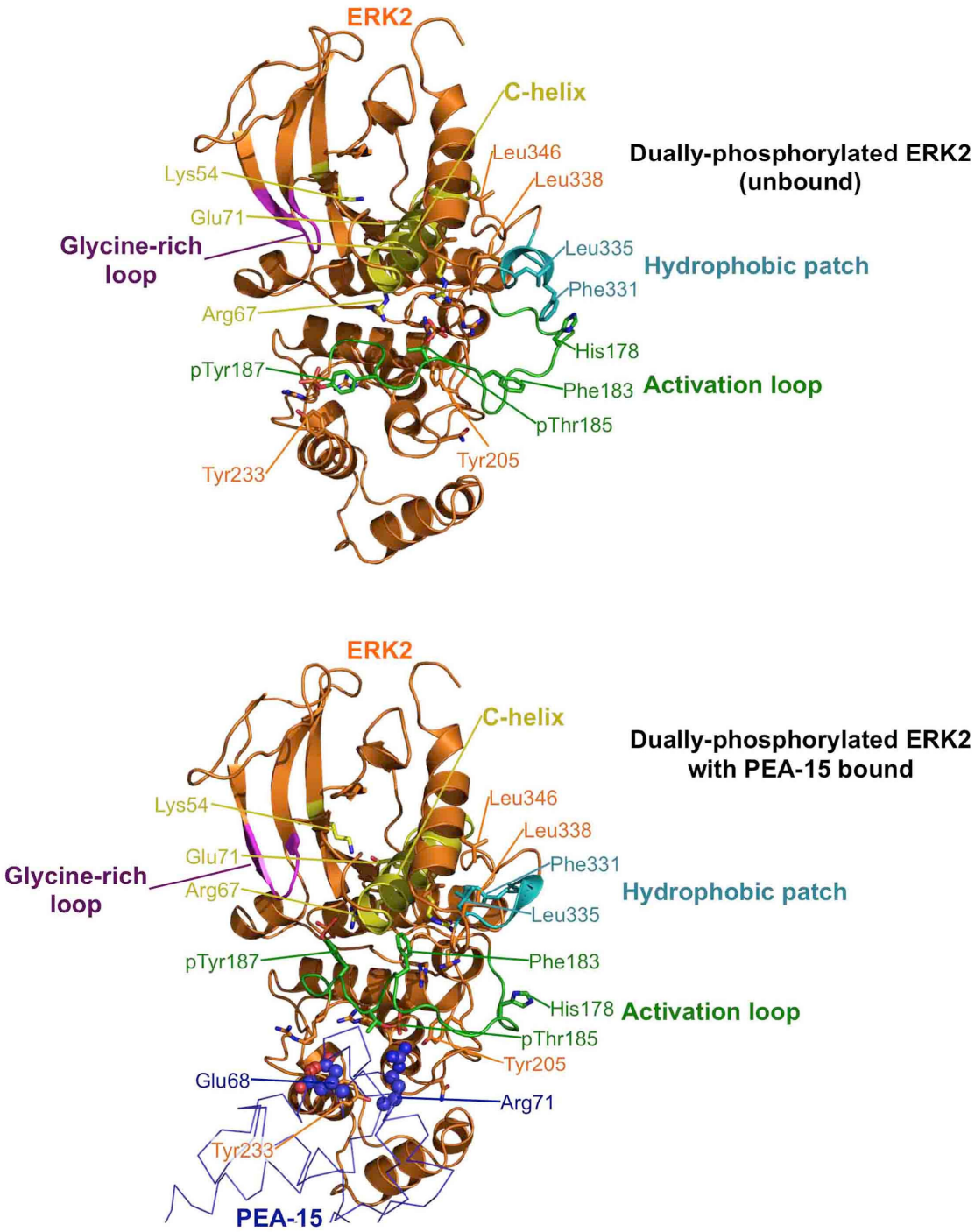

Supplementary Figure S7. Short and long range allosteric changes accompany binding of PEA-15 to dually phosphorylated ERK2. Displayed are the two ERK2 states also shown in the **Supplementary Movie**: dually phosphorylated ERK2 alone (orange, PDBid:2erk, top) and in the PEA-15-bound form (bottom). Residues of interest that are visualized in the accompanying **Supplementary Movie** are shown in stick representation and annotated (with the exception of arginine residues 70, 148, 172, 191 and 194, which form the phospho-binding pockets and are displayed but not annotated; residue numbering refers to human ERK2).

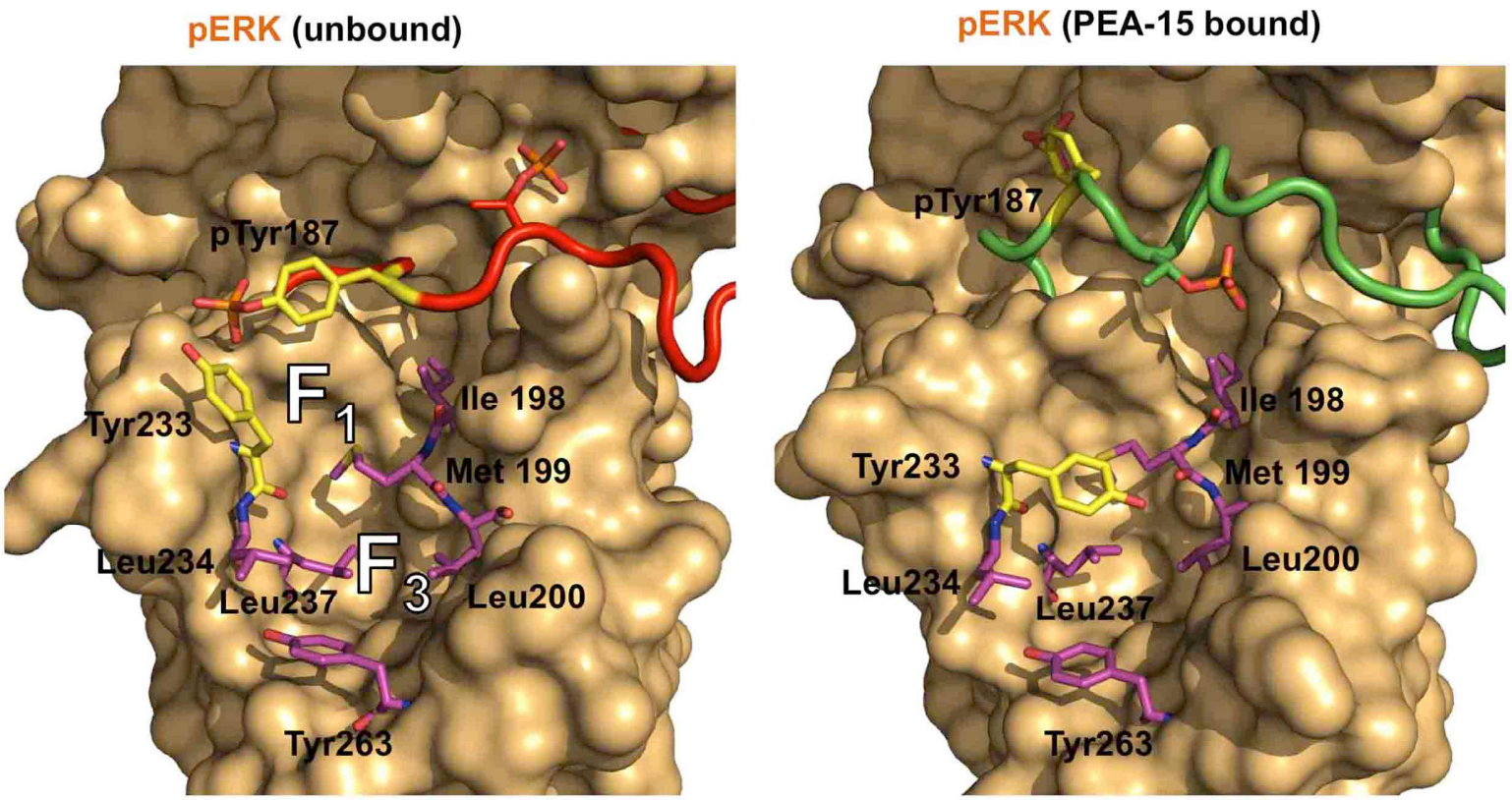

Supplementary Figure S8. Regulatory DEF-interaction and FXF-binding pockets. Unbound and PEA-15-bound ERK2 are displayed as in **Fig. 4b**. The residues forming the FXF binding pockets (indicated by F1 and F3) are depicted according to Sheridan *et. al.*[28]. These residues are displayed in stick representation and colored magenta except for residues Tyr 233 and pTyr187 which are colored yellow to highlight their profoundly different positions in unbound versus PEA-15-bound ERK2 (residue numbering refers to human ERK2).

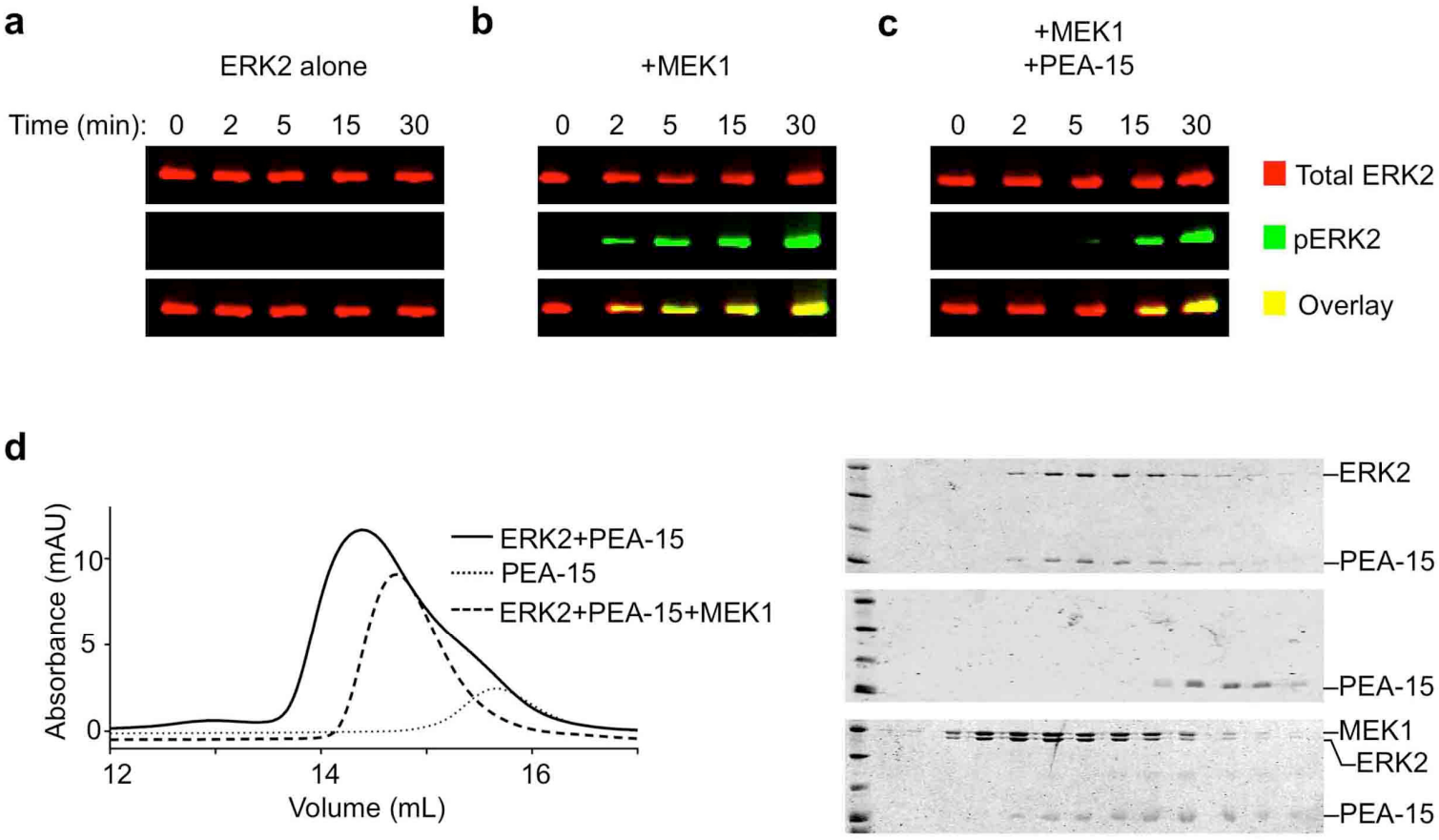

Supplementary Figure S9. PEA-15 is permissive for ERK2 phosphorylation by MEK1. (**a-c**) Time course of ERK2 activation by MEK1, comparing dually phosphorylated ERK2 and total ERK2 visualized using LICOR staining of Western blots. Concentrations used: 5 µM ERK2, 0.5 µM MEK1, 10 µM PEA-15. (**d**) ERK2-PEA-15 versus ERK2-MEK1 interaction at micromolar concentrations in an equimolar setting. Shown are gel filtration elution profiles (left) and SDS-PAGE analysis of fractions (right) from **Supplementary Figure S1c** featuring the PEA-15-ERK2 complex (top), PEA-15 alone (middle) in comparison to PEA-15, ERK2 and MEK1 (bottom) mixed at equimolar concentration (17 µM). The profile of the PEA-15-ERK2 complex is altered significantly in the presence of MEK1. A protein peak with an apparent molecular weight of 60 kDa appears, which contains mainly ERK2 and MEK1 while the majority of PEA-15 shifts to a smaller apparent molecular weight than observed for the PEA-15-ERK2 complex. This indicates that MEK at least partially displaces PEA-15 from ERK2 under high concentration conditions. These conditions may mimic MEK1-ERK2 signaling platforms formed in the presence of scaffolding proteins such as KSR.

SUPPLEMENTARY REFERENCES

52. Kornev, A. P. & Taylor, S. S. Defining the conserved internal architecture of a protein kinase. *Biochim Biophys Acta* **1804**, 440–444 (2010).